JACC: CARDIOVASCULAR IMAGING
VOL. 5, NO. 4, 2012

ISSN 1936-878X/$36.00
PUBLISHED BY ELSEVIER INC.
DOI:10.1016/j.jcmg.2011.10.004

ORIGINAL RESEARCH

Influence of Chronic Tethering of the Mitral Valve on Mitral Leaflet Size and Coaptation in Functional Mitral Regurgitation

Ken Saito, MD, Hiroyuki Okura, MD, Nozomi Watanabe, MD, Kikuko Obase, MD, Tomoko Tamada, MD, Terumasa Koyama, MD, Akihiro Hayashida, MD, Yoji Neishi, MD, Takahiro Kawamoto, MD, Kiyoshi Yoshida, MD

Kurashiki, Japan

OBJECTIVES The purposes of this study were to examine whether tethering of the mitral leaflets affects coaptation in patients with functional mitral regurgitation (FMR) and to assess the interaction between the mitral coaptation and mitral regurgitation severity.

BACKGROUND Functional mitral regurgitation causes restriction of leaflet closure as a result of enhanced tethering of the mitral leaflets and papillary muscle (PM) displacement.

METHODS Three-dimensional transesophageal echocardiography was performed in 44 patients with FMR related to the bilateral PM displacement and in 56 controls. The distance between the tip of the anterior or posterior PM and the intervalvular fibrosa were measured as the lateral or medial tethering length (TL) in midsystole. To evaluate the degree of coaptation, coaptation length (CL) at medial, middle, and lateral sites of mitral valve and an estimate of coaptation area (CA) were measured.

RESULTS The FMR group showed the significantly decreased CA (1.3 ± 0.4 cm^2 vs. 1.6 ± 0.4 cm^2, $p = 0.005$) and CL (medial 3.2 ± 0.9 mm vs. 4.8 ± 0.6 mm, middle 3.8 ± 1.3 mm vs. 5.8 ± 0.7 mm, lateral 3.3 ± 0.9 mm vs. 4.8 ± 0.6 mm; all $p < 0.0001$) compared with the controls. Each CL correlated negatively and significantly with both medial and lateral TL (all $p < 0.0001$). Annular area ($p = 0.004$) was significantly smaller and leaflet-to-annular area ratio ($p < 0.0001$) was significantly larger in patients with nonsignificant FMR than in the patients with significant (moderate to severe) FMR. Significant correlations were found between effective regurgitant orifice area and CA or each CL (all $p < 0.0001$).

CONCLUSIONS Coaptation decreased significantly in patients with FMR. The CL at each region was related to PM displacement and the indexes of coaptation were associated with mitral regurgitation severity. (J Am Coll Cardiol Img 2012;5:337–45) © 2012 by the American College of Cardiology Foundation

From the Department of Cardiology, Kawasaki Medical School, Kurashiki, Japan. All authors have reported they have no relationships relevant to the contents of this paper to disclose.

Manuscript received July 6, 2011; revised manuscript received September 28, 2011, accepted October 11, 2011.

Functional mitral regurgitation (FMR) typically occurs in patients with ischemic cardiomyopathy (ICM) and dilated cardiomyopathy (DCM) and is associated with excessive mortality (1–3). FMR causes restriction of leaflet closure as a result of dilation of the mitral annulus, enhanced tethering of the mitral valve (MV) leaflets, papillary muscles (PM) displacement, and reduced closing force of the leaflets without primary valve leaflet pathology (4–8).

See page 346

Recently, it has been suggested that leaflets may be elongated in response to stress imposed by increased tethering (9). It has been shown that patients with mitral leaflet tethering caused by DCM or inferior myocardial infarction have larger mitral leaflet areas than the controls with normal heart measured by 3-dimensional (3D) echocardiography (10). Therefore, patients with insufficient adaptation to the tethered valve geometry could have incomplete leaflet closure and more mitral regurgitation (MR). However, there was a limitation in evaluating regional mitral leaflet coaptation, and little is known about the interaction between MR severity and indexes of the coaptation. The recent development of 3D transesophageal echocardiography (TEE) made it possible to provide excellent images of MV apparatus and accurate measurements of the mitral complex (11,12) Our aims were: 1) to examine whether chronic tethering of the mitral leaflets affects MV size, coaptation area, and regional coaptation length in patients with FMR; and 2) to assess the interaction between indexes of the mitral coaptation and MR severity.

ABBREVIATIONS AND ACRONYMS

CA = coaptation area
CI = coaptation index
CL = coaptation length
DCM = dilated cardiomyopathy
EROA = effective regurgitant orifice area
FMR = functional mitral regurgitation
ICM = ischemic cardiomyopathy
LV = left ventricular
MR = mitral regurgitation
MV = mitral valve
PM = papillary muscle
TEE = transesophageal echocardiography
3D = 3-dimensional
TL = tethering length

METHODS

Patient population. Forty-four patients (age 68 ± 7 years, 38 men) with FMR related to bilateral PM displacement (n = 44; 18 with DCM, 26 with ICM) were recruited for 3D echocardiographic examination. In 26 patients with ICM, the infarct-related artery was the left anterior descending artery in 26 patients (100 %), the right coronary artery in 22 patients (85%), and the left circumflex artery in 20 patients (77 %). To clarify the determinants of MR, study patients were characterized as having significant (moderate or severe) MR, defined by the effective regurgitant orifice area (EROA) ≥ 0.2 cm^2 or nonsignificant MR if the EROA was <0.2 cm^2 based on recommendations by the American Society of Echocardiography (13). MR was quantified by the EROA calculated by either the proximal isovelocity surface area method or the quantitative pulse wave Doppler method using mitral and aortic stroke volumes (14). Fifty-six subjects (ages 67 ± 12 years, 31 men) who have no MR with normal left ventricular (LV) function and mitral apparatus were also examined as controls. Exclusion criteria were: 1) organic MV or subvalvular lesion (e.g., mitral leaflet prolapse or rheumatic disease); and 2) other cardiac diseases (e.g., pericardial, congenital, endocarditis, and aortic valve disease). The ethics committee of Kawasaki Medical School approved this study protocol.

Conventional echocardiographic examination. Two-dimensional transthoracic echocardiography was performed on patients in the left lateral decubitus position using a commercially available echocardiographic machine (iE33, Philips Medical Systems, Andover, Massachusetts) with a 5-MHz transducer. In the parasternal long-axis view, LV end-diastolic diameter, end-systolic diameter, and left atrial dimension were measured as reported previously. The LV end-diastolic volume, LV end-systolic volume, and LV ejection fraction were measured by a biplane method of disks in the apical 2- and 4-chamber views (15). The LV sphericity index was calculated as the short-axis diameter in mid-LV region divided by the long-axis diameter at end-systolic phase in the apical 4-chamber view.

3D TEE. MEASUREMENT OF MITRAL COMPLEX. 3D TEE was performed using the iE33 with an X7-2t matrix-array transducer (Philips Medical Systems). In the acquisition of 3D echocardiographic data of mitral complex, a 101° × 104° pyramid of gated full-volume mode over 4 beats was used for patients with normal sinus rhythm, and a 3D zoom mode was used for patients with atrial fibrillation. The 3D computer software REAL VIEW (YD Ltd., Nara, Japan) was used to analyze the mitral complex. As previously reported (8,16,17), the 3D data were automatically cropped into 18 radial planes oriented 10° apart (Fig. 1). The mitral annulus in each cropped plane was manually plotted, while the mitral leaflets were traced semiautomatically in each cropped plane. The tips of the PM were captured and marked on cropped planes. The 3D images of the mitral leaflets and annulus were reconstructed from the acquired data, showing the colored con-

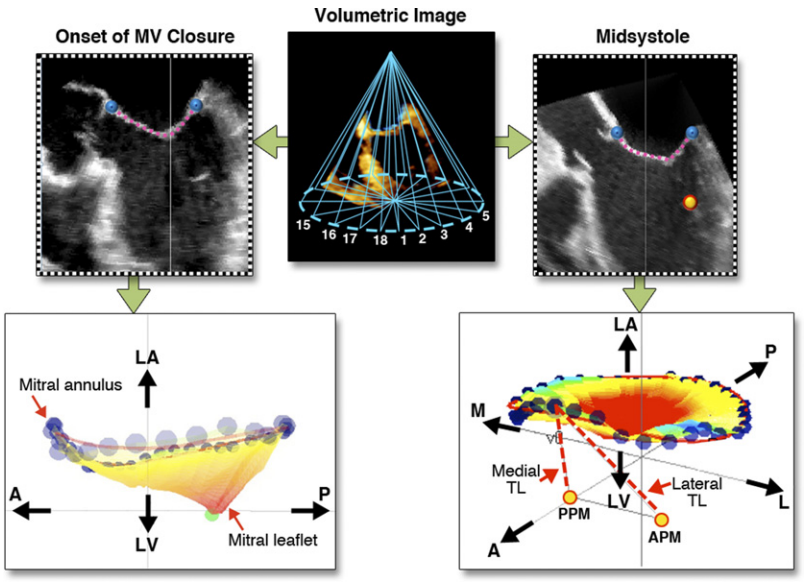

Figure 1. 3D Volumetric Image

This 3-dimensional (3D) volumetric image was automatically cropped into 18 equally spaced radial planes. The mitral valve (MV) annulus was marked **(blue dots)**, and the leaflets were traced **(pink dotted-line)** in each cropped plane. The tips of the posterior papillary muscle (PPM) and anterior papillary muscle (APM) were obtained and marked **(yellow dot)**. The 3D images of the mitral complex apparatus were anatomically reconstructed for the quantitative measurements **(bottom)**. The leaflet area was assessed at the onset of mitral leaflet closure **(left)**, and the annular area, the tenting volume, and the tethering length (TL) were in midsystole **(right)**. A = anterior side; L = lateral side; LA = left atrium; LV = left ventricle; M = medial side; P = posterior side.

figuration of the leaflet curvature and curved annulus, with an alignment of PM tips (Fig. 1). The total leaflet area was assessed at the onset of mitral leaflet closure. The mitral annular area was calculated at midsystole. The tenting volume was calculated as the volume enclosed between the estimated curved annular surface and mitral leaflets at midsystole. To observe the PM displacement, we measured the distance between the tip of the anterior or posterior PM and intervalvular fibrosa (the middle anterior part of the annulus) as the lateral or medial tethering length (TL) in mid systole (Fig. 1). All the measurement values were normalized to body surface area.

MEASUREMENT OF COAPTATION. The 3D data sets were digitally stored and transferred to a workstation with Q-Lab software (Philips Medical Systems) with 3D-Q plug-in for offline analysis. Three simultaneous orthogonal mitral annulus planes and a fourth view showing the orientation of the planes related to volume were presented in multiplanar reformatting mode (Fig. 2) (18). Within each of the planar views, the location of intersection with other imaging planes was shown by reference lines, which could be moved to change the orientation and the intersection with other planes. The coaptation length (CL) at the medial, middle, and lateral sites were measured on the optimal long-axis cut plane at midsystole with multiplanar reformatting mode (Fig. 3). The middle site was determined as the center of the MV. Then, the medial site was specified as the center of the medial half of the MV. Similarly, the lateral site was specified as the center of the lateral half of the MV. To visualize leaflet coaptation as clearly as possible, the gain was adjusted optimally. Because it was difficult to measure the coaptation length individually due to limited lateral resolution, only the longest coaptation length was measured in this study. Interobserver variabilities of the value of the CL evaluated by means of intraclass correlation coefficients were 0.94 at medial, 0.91 at middle, and 0.96 at lateral lesion. Coaptation area (CA) data were acquired with REAL VIEW (YD Ltd.), and CA evaluated by the following calculation: CA = total leaflet area − closed leaflet area in midsystole (Fig. 4). Total leaflet area was calculated at the onset of mitral leaflet closure in this study. However, it has been demonstrated the mitral leaflet stretches during systole (19,20). Therefore, total systolic leaflet area could be underestimated, leading to the underestimation of CA. Additionally, the coaptation index (CI) was calculated as the ratio

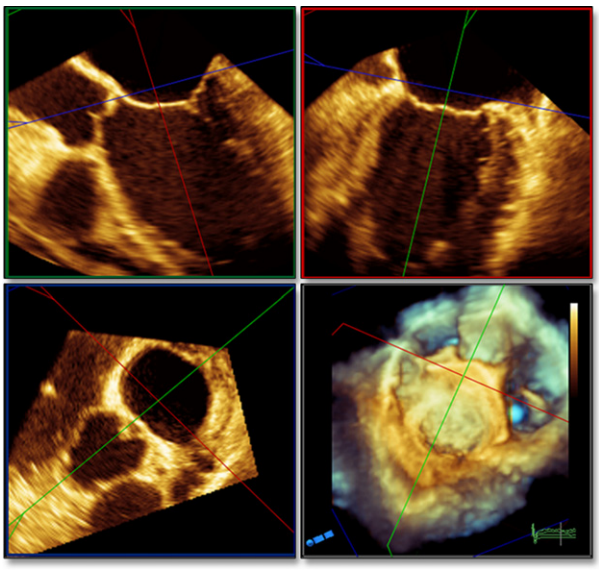

Figure 2. Multiple Simultaneous Orthogonal Slices

Multiple simultaneous orthogonal 2-dimensional–like slices can be presented in multiplanar reformatting mode. The **red plane** and **green plane** show long-axis cut planes, and the **blue plane** presents short-axis cut plane parallel to the mitral annulus.

of CA to total leaflet area by the following formula: CI = (total leaflet area − closed leaflet area in midsystole)/total leaflet area × 100 (Fig. 4) (8).

Statistical analysis. Categorical variables were presented as counts and percentages and compared with the chi-square test. Continuous variables were presented as mean values ± SD. Statistical analysis was performed using the 2-sample unpaired *t* test for normally distributed data, and the Mann-Whitney *U* test was used for data that were not normally distributed after testing the normality of the data with the Saphiro-Wilks test. For continuous variables, analysis of variance with post-hoc analysis using the Scheffé test was used to differentiate among 3 regions. The association between the CL and the indexes of LV apparatus was investigated with the linear regression analysis. Correlations between EROA and indexes of coaptation were analyzed by the Spearman rank-order correlation. A p value <0.05 was considered statistically significant. Statistical analysis was performed using SPSS (SPSS, Chicago, Illinois) and Statview (SAS Institute, Cary, North Carolina).

RESULTS

Patient characteristics and 2-dimensional echocardiographic parameters are summarized in Table 1. There were no differences in age, sex, and body surface area between those groups. The LV dimen-

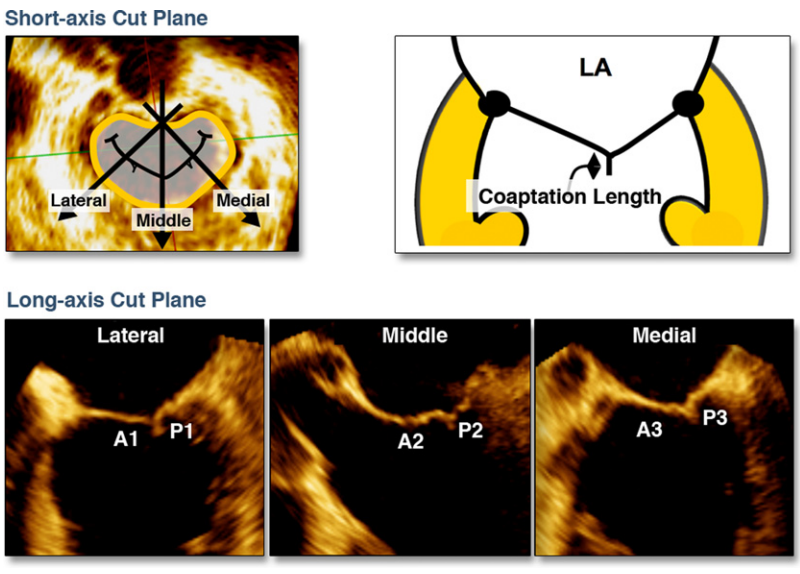

Figure 3. Measurement of Coaptation Length Using MPR Slice Display

Measurement of coaptation length **(top right)** using multiplanar reformatting (MPR) slice display. By moving and rotating cut planes on cross-sectional volumetric image at mitral annulus level **(top left)**, the optimal long-axis cut planes **(bottom)** were selected to allow analysis of coaptation length at the lateral, middle, and medial sites. A1 = lateral segment of the anterior mitral leaflet; A2 = middle segment of the anterior mitral leaflet; A3 = medial segment of the anterior mitral leaflet; P1 = lateral scallop of the posterior mitral leaflet; P2 = middle scallop of the posterior mitral leaflet; P3 = medial scallop of the posterior mitral leaflet. Abbreviation as in Figure 1.

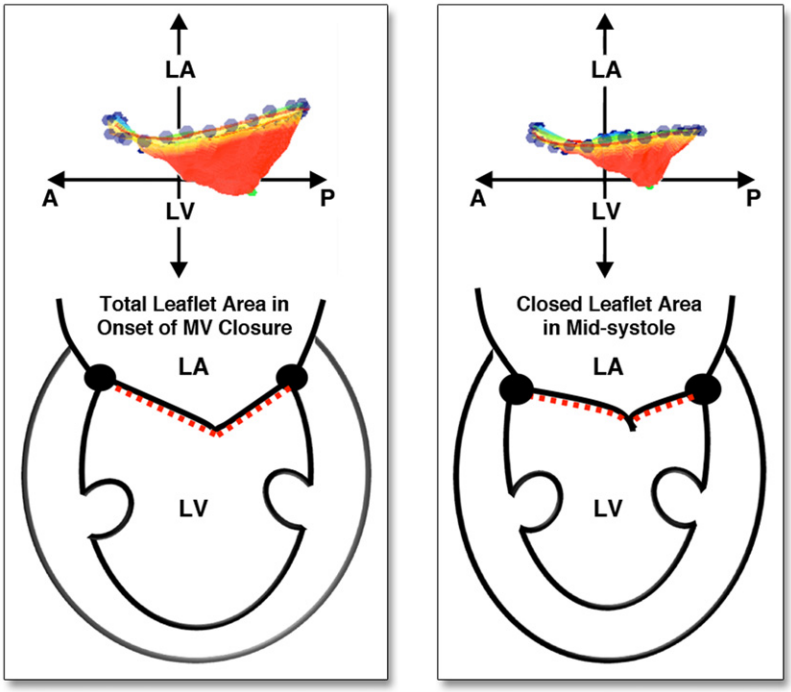

Figure 4. MV Apparatus Geometry

MV apparatus geometry in the onset of mitral leaflet closure **(left)** and the timing of maximum closure of mitral leaflet **(right)**. The 3-dimensional tenting closed leaflet area does not include coapted leaflet area in this study. Abbreviations as in Figure 1.

sions, LV volumes, and left atrial dimension were significantly larger and LV ejection fractions were lower in the FMR group compared with those in the control group (all $p < 0.0001$). The elliptical shape of LV becomes more spherical in patients with FMR than in the control subjects ($p < 0.0001$).

Mitral complex geometry and leaflet coaptation. The mitral complex geometry and leaflet coaptation indexes are summarized in Table 2. The mitral annular area, tenting volume, and TL were significantly larger in patients with FMR than in the control subjects (all $p < 0.0001$). The leaflet area showed similar increase in patients with FMR ($p < 0.0001$); however, there were no significant difference in leaflet-to-annular area ratio between the 2 groups ($p = 0.09$).

In the control group, the CL at the middle site was significantly longer than that at the medial and lateral sites. In contrast, in the FMR group, there were no significant differences among the 3 regions. In patients with LV remodeling, the CL at all 3 sites significantly (all $p < 0.0001$) and proportionally decreased compared with those in the controls. The CA and CI in patients with FMR were also significantly smaller than those in the control subjects ($p = 0.005$ and $p < 0.0001$, respectively).

Because the loss of coaptation was considered as the phenomenon secondary to the PM displacement and annular dilation, we assessed the relationship between CL and TL. The correlations between

Table 1. Patients' Clinical and 2-Dimensional Echocardiographic Characteristics

	FMR Group (n = 44)	Control Group (n = 56)	p Value
Men	38 (86)	31 (55)	0.10
Age, yrs	68 ± 7	67 ± 12	0.62
Body surface area, m^2	1.6 ± 0.1	1.6 ± 0.2	0.94
2-Dimensional echocardiography			
Left ventricle			
Diastolic dimension, mm	60 ± 6	44 ± 3	<0.0001
Systolic dimension, mm	51 ± 8	28 ± 4	<0.0001
Diastolic volume, ml	164 ± 41	91±11	<0.0001
Systolic volume, ml	112 ± 39	31 ± 10	<0.0001
Ejection fraction, %	33 ± 11	66 ± 7	<0.0001
Sphericity index	0.59 ± 0.06	0.39 ± 0.05	<0.0001
Left atrial dimension, mm	59 ± 11	35 ± 4	<0.0001
Regurgitant orifice area, cm^2	0.27 ± 0.19	—	—

Values are n (%) or mean ± SD.
FMR = functional mitral regurgitation.

Table 2. Geometric Measurements of Mitral Complex and Coaptation

	FMR Group (n = 44)	Control Group (n = 56)	p Value
Annular area, cm^2/m^2	6.0 ± 2.5	4.5 ± 0.6	<0.0001
Leaflet area, cm^2/m^2	8.7 ± 1.8	6.7 ± 0.9	<0.0001
Leaflet to annular area ratio	1.45 ± 0.16	1.50 ± 0.11	0.09
Tenting volume, ml/m^2	1.3 ± 0.7	0.5 ± 0.3	<0.0001
Tethering length, mm/m^2			
Medial	23.0 ± 2.2	18.4 ± 2.8	<0.0001
Lateral	20.5 ± 3.2	17.1 ± 2.6	<0.0001
Coaptation length, mm			
Medial	3.2 ± 0.9	4.8 ± 0.6	<0.0001
Middle	3.8 ± 1.3	5.8 ± 0.7*†	<0.0001
Lateral	3.3 ± 0.9	4.8 ± 0.6	<0.0001
Coaptation area, cm^2/m^2	1.3 ± 0.4	1.6 ± 0.4	0.005
Coaptation index, %	15.6 ± 3.3	23.6 ± 4.8	<0.0001

Values are mean ± SD. *p < 0.05 versus medial. †p < 0.05 versus lateral.
Abbreviation as in Table 1.

the CL at all 3 sites and the medial TL were negative and significant (Figs. 5A to 5C) (medial $r = 0.55$, $p < 0.0001$; middle $r = 0.57$, $p < 0.0001$; lateral $r = 0.54$, $p < 0.0001$). The correlation between the CL and lateral TL was similarly negative and significant (medial $r = 0.45$, $p < 0.0001$; middle $r = 0.51$, $p < 0.0001$; lateral $r = 0.55$, $p < 0.0001$) (Figs. 5D to 5F). Additionally, the leaflet-to-annular area ratio correlated positively and significantly with regional CLs (medial $r = 0.47$, $p < 0.0001$; middle $r = 0.68$, $p < 0.0001$; lateral $r = 0.51$, $p < 0.0001$).

Significant FMR versus nonsignificant FMR. There were no differences in LV volumes, tethering length, and tenting volume between patients with and without significant FMR in this study population (Table 3). There was also no difference in leaflet area between the 2 groups ($p = 0.64$). Conversely, the annular area was significantly smaller in patients with significant FMR compared with the patients without significant FMR ($p = 0.004$). Therefore, leaflet-to-annular area ratio in patients with significant FMR was smaller than that in patients without significant FMR ($p < 0.0001$), suggesting that annular dilation and insufficient leaflet adaptation to the chronic tethering in patients with global LV remodeling leads to significant FMR. Actually, the coaptation indexes including CL, CA, and CI decreased in patients with FMR (all $p < 0.0001$).

DCM versus ICM. The measurements of 3D mitral complex geometry and leaflet coaptation were analyzed separately for patients with DCM (n = 18) and ICM (n = 26). There was no difference in EROA between the 2 groups (0.28 ± 0.2 cm^2 vs. 0.26 ± 0.2 cm^2, $p = 0.66$). Also, no significant differences in the measurements of 3D mitral complex geometry and leaflet coaptation were found between the 2 groups (Table 4).

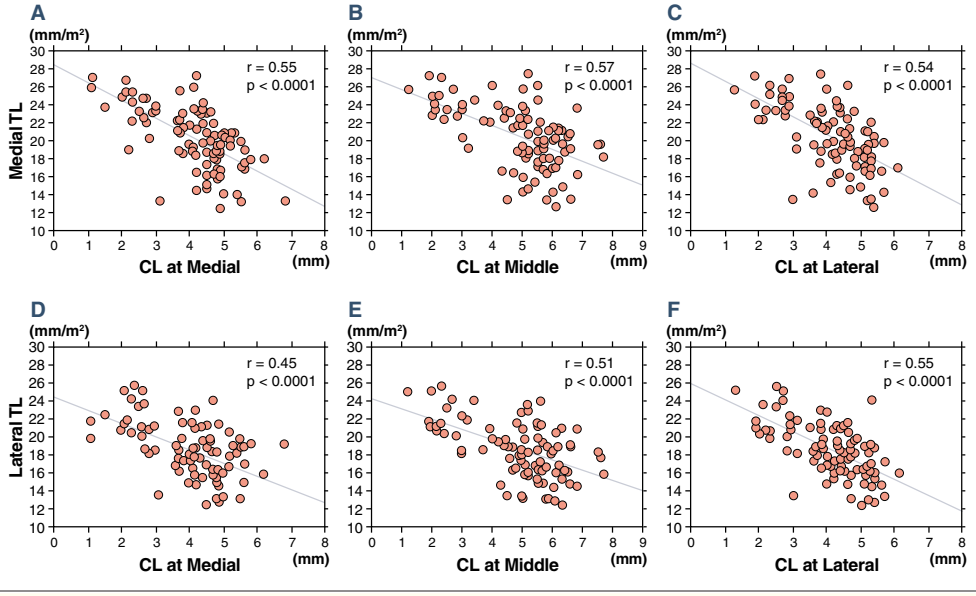

Figure 5. Correlations Between CL and TL

Negative and significant correlations ($p < 0.0001$) were found between coaptation length (CL) measured on the medial **(A)**, middle **(B)**, and lateral sites **(C)** and the medial tethering length (TL). The correlations between CL on the medial **(D)**, middle **(E)**, and lateral sites **(F)** and the lateral TL were similarly negative and significant.

Correlations between leaflet coaptation and MR severity. Spearman rank-order correction analysis showed a significant correlation between EROA and CA ($\rho = -0.76$, $p < 0.0001$) or CI ($\rho = -0.73$, $p < 0.0001$). The medial CL ($\rho = -0.73$, $p < 0.0001$), middle CL ($\rho = -0.76$, $p < 0.0001$), and lateral CL ($\rho = -0.73$, $p < 0.0001$) were also associated with EROA.

DISCUSSION

Our study shows that: 1) the mitral leaflet coaptation decreased proportionally in patients with FMR related to the bilateral PM displacement, despite increased total leaflet area to compensate for the increased mitral annular area and mitral leaflet tethering; 2) annular area was significantly smaller and leaflet-to-annular area ratio was significantly larger in patients with global LV remodeling who have nonsignificant FMR compared with the patients with significant FMR; and 3) the indexes of coaptation were related to MR severity.

FMR is produced by a complex combination of pathophysiological processes where distorted and spherical LV geometry leads to tethering of the chordae and therefore incomplete leaflet coaptation (8,10,21). In this condition, patients with mitral leaflet tethering have been shown to have larger mitral leaflet area than the control subjects (10). Similarly, Dal-Bianco et al. (22) demonstrated that mechanical stresses imposed by PM tethering increased MV leaflet area and matrix thickness, with cellular changes suggestive of reactivated embryonic valve development pathways. Therefore, patients with greater valve adaptation to the tethered valve geometry could have more complete leaflet closure and less MR. In our study population, significant MR was observed, despite the enlargement of the leaflet size and the preserved compensated mitral leaflet-to-annular area ratio.

Compared with the patients who had significant FMR, annular area was significantly smaller and leaflet-to-annular area ratio was larger in patients with LV remodeling and global systolic dysfunction who did not have significant FMR. This may be a result of decreased systolic annular contraction and/or inadequate leaflet adaptation to the annular dilation and leaflet tethering caused by the distorted LV geometry, concordant with a previous report (10). Actually, the CLs at all 3 regions decreased significantly in patients with significant FMR than in patients without FMR.

Table 3. Echocardiographic Characteristics of Patients With and Without Significant FMR

	Significant FMR (n = 24)	Nonsignificant FMR (n = 20)	p Value
Diastolic volume, ml	168 ± 43	161 ± 38	0.51
Systolic volume, ml	110 ± 42	113 ± 37	0.62
Regurgitant orifice area, cm^2	0.44 ± 0.14	0.12 ± 0.03	<0.0001
Annular area, cm^2/m^2	6.8 ± 1.6	5.4 ± 0.9	0.004
Leaflet area, cm^2/m^2	9.2 ± 1.9	8.3 ± 1.6	0.64
Leaflet to annular area ratio	1.35 ± 0.15	1.53 ± 0.12	<0.0001
Tenting volume, ml/m^2	1.5 ± 0.7	1.2 ± 0.6	0.14
Tethering length, mm/m^2			
Medial	23.2 ± 2.3	22.6 ± 1.7	0.08
Lateral	20.8 ± 2.3	19.9 ± 1.7	0.06
Coaptation length, mm			
Medial	2.4 ± 0.5	3.9 ± 0.7	<0.0001
Middle	2.8 ± 1.0	4.7 ± 1.1	<0.0001
Lateral	2.6 ± 0.6	3.9 ± 0.6	<0.0001
Coaptation area, cm^2/m^2	0.9 ± 0.3	1.6 ± 0.4	<0.0001
Coaptation index, %	10.4 ± 3.5	20.1 ± 5.5	<0.0001

Values are mean ± SD.
Abbreviation as in Table 1.

Previous studies using 3D transthoracic echocardiography reported that the degree of mitral valve coaptation in patients with FMR was significantly smaller than that in normal subjects (8,10). Another group demonstrated that the symmetrical papillary muscle displacement led to progressive chordal tethering and decreased coaptation in patients with global LV dysfunction, resulting in predominantly central MR (23,24). In the present study, such decrease in coaptation occurred proportionately and the CL correlated significantly with the displacement of PMs.

Table 4. The Geometry of Mitral Complex in Patients With DCM and ICM

	DCM (n = 18)	ICM (n = 26)	p Value
Annular area, cm^2/m^2	6.2 ± 1.5	5.8 ± 1.4	0.30
Leaflet area, cm^2/m^2	8.8 ± 1.8	8.5 ± 1.8	0.55
Leaflet to annular area ratio	1.42 ± 0.16	1.47 ± 0.18	0.21
Tenting volume, ml/m^2	1.4 ± 0.8	1.3 ± 0.5	0.31
Tethering length, mm/m^2			
Medial	23.1 ± 2.2	23.0 ± 2.2	0.78
Lateral	20.4 ± 1.9	20.5 ± 2.6	0.88
Coaptation length, mm			
Medial	3.1 ± 1.1	3.3 ± 1.1	0.52
Middle	3.6 ± 1.6	3.9 ± 1.3	0.33
Lateral	3.1 ± 1.0	3.4 ± 0.8	0.28
Coaptation area, cm^2/m^2	1.4 ± 0.7	1.3 ± 0.4	0.97
Coaptation index, %	15.9 ± 8.9	15.4 ± 4.6	0.82

Values are mean ± SD.
DCM = dilated cardiomyopathy; ICM = ischemic cardiomyopathy.

In addition, we observed that the CL at medial, middle, and lateral sites, CA, and CI were associated with the MR severity. To further preserve the mitral valvular coaptation, extension of the mitral leaflet for patients with FMR has been successfully performed in the clinical setting (25,26). In cases of progressive ventricular remodeling, however, this reconstructive surgical procedure for the MV has shown limited efficacy. Therefore, surgical procedures targeting the subvalvular apparatus and LV may be required.

Clinical implications. A considerable number of patients with ischemic MR could often present with persistent or recurrent MR even after undersized ring annuloplasty (27–30). Such failures of ring annuloplasty emphasize the necessity of procedures targeting the subvalvular apparatus. Recently, Langer et al. (31) reported that the annuloplasty ring plus posterior PM repositioning procedure clinically treated ischemic MR better than an undersized annuloplasty ring alone. However, as suggested in our study and the previous report (17), tethered leaflet in patients with bilateral PM displacement is usually observed not only on the medial side but also on the lateral side, which may necessitate more physiological "chordal relocation" where both papillary heads are repositioning to the annulus (32–34). Therefore, a comprehensive preoperative assessment including the measurements of the mitral complex and CLs at 3 sites may contribute to the reconstruction of the mitral complex and LV physiologic geometry.

Study limitations. Our study has limitations in that it has a lack of patients with regional LV remodeling (e.g., isolated inferior wall-motion abnormality). Therefore, prospective studies are needed to clarify the relationship between the coaptation length and mitral complex apparatus in those patients. Total leaflet area was calculated at the onset of mitral leaflet closure in this study. However, it has been demonstrated that the mitral leaflet stretches during systole (20,21). Therefore, total leaflet area could be underestimated, leading to the underestimation of CA. However, it is not anticipated that will change the relation between measures of coaptation and functional MR outcome.

CONCLUSIONS

Despite the increased mitral leaflet size to compensate for the increased mitral leaflet tethering, coaptation decreased significantly in patients with significant FMR. The regional coaptation was related to PM displacement, and the indexes of coaptation were related to MR severity. These results may have implications for surgical strategy for individual patients with FMR.

Acknowledgments

The authors thank their research staff and technologists at the cardiovascular core analysis laboratory.

Reprint requests and correspondence: Dr. Hiroyuki Okura, Department of Cardiology, Kawasaki Medical School, 577 Matsushima, Kurashiki 701-0192, Japan. *E-mail: hokura@fides.dti.ne.jp.*

REFERENCES

1. Junker A, Thayssen P, Nielsen B, et al. The hemodynamic and prognostic significance of echo-Doppler-proven mitral regurgitation in patients with dilated cardiomyopathy. Cardiology 1993;83:14–20.
2. Grigioni F, Enriquez-Sarano M, Zehr KJ, et al. Ischemic mitral regurgitation: long-term outcome and prognostic implications with quantitative Doppler assessment. Circulation 2001;103:1759–64.
3. Okura H, Takada Y, Kubo T, et al. Functional mitral regurgitation predicts prognosis independent of left ventricular systolic and diastolic indices in patients with ischemic heart disease. J Am Soc Echocardiogr 2008; 21:355–60.
4. Hueb AC, Jatene FB, Moreira LF, et al. Ventricular remodeling and mitral valve modifications in dilated cardiomyopathy: new insights from anatomic study. J Thorac Cardiovasc Surg 2002;124:1216–24.
5. Otsuji Y, Handschumacher MD, Liel-Cohen N, et al. Mechanism of ischemic mitral regurgitation with segmental left ventricular dysfunction: 3-dimensional echocardiographic studies in models of acute and chronic progressive regurgitation. J Am Coll Cardiol 2001;37:641–8.
6. Otsuji Y, Kumanohoso T, Yoshifuku S, et al. Isolated annular dilation does not usually cause important functional mitral regurgitation: comparison between patients with lone atrial fibrillation and those with idiopathic or ischemic cardiomyopathy. J Am Coll Cardiol 2002;39:1651–6.
7. Kumanohoso T, Otsuji Y, Yoshifuku S, et al. Mechanism of higher incidence of ischemic mitral regurgitation in patients with inferior myocardial infarction: quantitative analysis of left ventricular and mitral valve geometry in 103 patients with prior myocardial infarction. J Thorac Cardiovasc Surg 2003;125:135–43.
8. Tsukiji M, Watanabe N, Yamaura Y, et al. Three-dimensional quantitation of mitral valve coaptation by a novel software system with transthoracic real-time three-dimensional echocardiography. J Am Soc Echocardiogr 2008;21:43–6.
9. Grande-Allen KJ, Borowski AG, Troughton RW, et al. Apparently normal mitral valves in patients with heart failure demonstrate biochemical and structural derangements: an extracellular matrix and echocardiographic study. J Am Coll Cardiol 2005;45:54–61.
10. Chaput M, Handschumacher MD, Tournoux F, et al. Mitral leaflet

adaptation to ventricular remodeling: occurrence and adequacy in patients with functional mitral regurgitation. Circulation 2008;118:845–52.

11. Sugeng L, Shernan SK, Salgo IS, et al. Live 3-dimensional transesophageal echocardiography initial experience using the fully-sampled matrix array probe. J Am Coll Cardiol 2008;52: 446–9.
12. Gogoladze G, Dellis SL, Donnino R, et al. Analysis of the mitral coaptation zone in normal and functional regurgitant valves. Ann Thorac Surg 2010; 89:1158–61.
13. Zoghbi WA, Enriquez-Sarano M, Foster E, et al. Recommendations for evaluation of the severity of native valvular regurgitation with two-dimensional and Doppler echocardiography. J Am Soc Echocardiogr 2003;16:777–802.
14. Rokey R, Sterling LL, Zoghbi WA, et al. Determination of regurgitant fraction in isolated mitral or aortic regurgitation by pulsed Doppler two-dimensional echocardiography. J Am Coll Cardiol 1986;7:1273–8.
15. Lang RM, Bierig M, Devereux RB, et al. Recommendations for chamber quantification: a report from the American Society of Echocardiography's Guidelines and Standards Committee and the Chamber Quantification Writing Group. J Am Soc Echocardiogr 2005;18:1440–63.
16. Watanabe N, Ogasawara Y, Yamaura Y, et al. Mitral annulus flattens in ischemic mitral regurgitation: geometric differences between inferior and anterior myocardial infarction: a real-time 3-dimensional echocardiographic study. Circulation 2005;112 Suppl 1:458–62.
17. Watanabe N, Ogasawara Y, Yamaura Y, et al. Quantitation of mitral valve tenting in ischemic mitral regurgitation by transthoracic real-time three-dimensional echocardiography. J Am Coll Cardiol 2005;45:763–9.
18. Beraud AS, Schnittger I, Miller DC, et al. Multiplanar reconstruction of three-dimensional transthoracic echocardiography improves the presurgical assessment of mitral prolapse. J Am Soc Echocardiogr 2009;22:907–13.
19. Chen L, May-Newman K. Effect of strut chordae transection on mitral valve leaflet biomechanics. Ann Biomed Eng 2006;34:917–26.
20. Chen L, McCulloch AD, May-Newman K. Nonhomogeneous deformation in the anterior leaflet of the mitral valve. Ann Biomed Eng 2004; 32:1599–606.
21. Kaul S, Spotnitz WD, Glasheen WP, et al. Mechanism of ischemic mitral regurgitation. An experimental evaluation. Circulation 1991;84:2167–80.
22. Dal-Bianco JP, Aikawa E, Bischoff J, et al. Active adaptation of the tethered mitral valve: insights into a compensatory mechanism for functional mitral regurgitation. Circulation 2009; 120:334–42.
23. Veronesi F, Corsi C, Sugeng L, et al. Quantification of mitral apparatus dynamics in functional and ischemic mitral regurgitation using real-time 3-dimensional echocardiography. J Am Soc Echocardiogr 2008;21:347–54.
24. Kwan J, Shiota T, Agler DA, et al. Geometric differences of the mitral apparatus between ischemic and dilated cardiomyopathy with significant mitral regurgitation: real-time three-dimensional echocardiography study. Circulation 2003;107:1135–40.
25. Kincaid EH, Riley RD, Hines MH, et al. Anterior leaflet augmentation for ischemic mitral regurgitation. Ann Thorac Surg 2004;78:564–8.
26. de Varennes B, Chaturvedi R, Sidhu S, et al. Initial results of posterior leaflet extension for severe type IIIb ischemic mitral regurgitation. Circulation 2009;119:2837–43.
27. Kuwahara E, Otsuji Y, Iguro Y, et al. Mechanism of recurrent/persistent ischemic/functional mitral regurgitation in the chronic phase after surgical annuloplasty: importance of augmented posterior leaflet tethering. Circulation 2006; 114 Suppl 1:529–34.
28. McGee EC, Gillinov AM, Blackstone EH, et al. Recurrent mitral regurgitation after annuloplasty for functional ischemic mitral regurgitation. J Thorac Cardiovasc Surg 2004;128:916–24.
29. Milano CA, Daneshmand MA, Rankin JS, et al. Survival prognosis and surgical management of ischemic mitral regurgitation. Ann Thorac Surg 2008;86:735–44.
30. Glower DD, Tuttle RH, Shaw LK, et al. Patient survival characteristics after routine mitral valve repair for ischemic mitral regurgitation. J Thorac Cardiovasc Surg 2005;129:860–8.
31. Langer F, Kunihara T, Hell K, et al. RING+STRING: Successful repair technique for ischemic mitral regurgitation with severe leaflet tethering. Circulation 2009;120 Suppl 1:85–91.
32. Arai H, Itoh F, Someya T, Oi K, Tamura K, Tanaka H. New surgical procedure for ischemic/functional mitral regurgitation: mitral complex remodeling. Ann Thorac Surg 2008;85: 1820–2.
33. Masuyama S, Marui A, Shimamoto T, et al. Chordal translocation for ischemic mitral regurgitation may ameliorate tethering of the posterior and anterior mitral leaflets. J Thorac Cardiovasc Surg 2008;136:868–75.
34. Masuyama S, Marui A, Shimamoto T, et al. Chordal translocation: secondary chordal cutting in conjunction with artificial chordae for preserving valvular-ventricular interaction in the treatment of functional mitral regurgitation. J Heart Valve Dis 2009;18: 142–6.

Key Words: functional mitral regurgitation ■ left ventricular remodeling ■ mitral valve coaptation ■ 3-dimensional transesophageal echocardiography.